

Structural and Electrical Properties of $\text{Ru}_{0.9}\text{M}_{0.1}\text{Sr}_2\text{GdCu}_2\text{O}_8$ System With $\text{M} = \text{Zr}, \text{Mo}, \text{AND Mn}$

M. Abatal^{1*}, A. Gonzalez-Parada², A. Quiroz¹, S. Diaz-Mendez¹, H. Alazki¹, V. García-Vázquez³ and E. Chavira⁴

* mabatal@pampano.unacar.mx

Received: April 2018 Revised: November 2018 Accepted: January 2019

¹ Facultad de Ingeniería, Universidad Autónoma del Carmen, Cd del Carmen, Campeche, México.

² University of Guanajuato, León, México

³ Instituto de Física Luis Rivera Terrazas, Benemérita Universidad Autónoma de Puebla, Puebla, México.

⁴ Instituto de Investigaciones en Materiales, UNAM, México, Cd. Mx., México.

DOI: 10.22068/ijmse.16.1.61

Abstract: The superconducting properties of the $\text{RuSr}_2\text{GdCu}_2\text{O}_8$ ceramic system depend strongly on the synthesis conditions and the ionic substitutions. In this work, we studied the structural and electrical properties of the $\text{Ru}_{0.9}\text{M}_{0.1}\text{Sr}_2\text{GdCu}_2\text{O}_8$ system, with $\text{M} = \text{Zr}, \text{Mo}, \text{and Mn}$. The samples were prepared by solid-state reaction at ambient pressure in air, using temperatures between 980 °C and 1020 °C. X-ray powder diffraction patterns indicated that all samples crystallized in a tetragonal symmetry (S.G. P4/mmm, No. 123). The structural data of each sample was refined by the Rietveld method, showing that the Cu-O (1) and Ru-O (1) bond lengths varies with the substituted ionic radii of Zr, Mo, and Mn ions. Electrical resistance measurements indicated that the samples annealed in flowing oxygen at 1050 °C and 1055 °C for 5 days exhibit a semiconductor like behavior for $\text{M} = \text{Mo}$ and Mn , whereas the samples with $\text{M} = \text{Zr}$ and Ru show superconductivity behavior.

Keywords: Rutheno-cuprates, XRD, Electric resistivity

1. INTRODUCTION

The rutheno-cuprates $\text{RuSr}_2\text{GdCu}_2\text{O}_8$ (Ru-1212) and $\text{RuSr}_2(\text{R}_{1-x}\text{Ce}_{1-x})\text{Cu}_2\text{O}_{10}$ ($\text{R} = \text{Sm}, \text{Eu}$ and Gd) are novel materials in which ferromagnetism and superconductivity coexists over a wide range of temperature [1]. Bauernfeind et al. [2] synthesized Ru-1212 compound for the first time and Felner et al. [3] discovered the extraordinary coexistence of both magnetism and superconductivity in these compounds two years later. The Ru-1212 layered cuprate exhibits a layered triple perovskite similar to the $\text{YBa}_2\text{Cu}_3\text{O}_7$ system, with Ba^{2+} and Y^{3+} replaced by Sr^{2+} and Gd^{3+} , respectively, and containing RuO_2 planes instead of the CuO chains in the blocking region of the structure [4]. Prior investigations showed that Ru-1212 material exhibit ferromagnetic ordering of the Ru moments on a microscopic scale below 133 K and becomes superconducting at a lower temperature between $T_c = 16$ K and 46 K depending on the sample preparation [5]. In order to investigate the origin of superconductivity and magnetism phe-

nomena and their relationship in the rutheno-cuprates compounds, previous reports have studied the effect of total or partial cation substitution in $\text{Ru}_{1-x}\text{M}_x\text{Sr}_2\text{GdCu}_2\text{O}_8$ system with $\text{M} = \text{Ce}$ [6], Ti [7, 8], Rh [8], Nb [7], V [7], Ir [9], Ta [10], Fe [11], Cu [12], and Co [13]. These studies reported that, the magnetic ordering and the superconducting transition temperatures are very sensitive to the synthesis process and depend on the type and concentration of the cation substitution.

In this paper, the partial substitution of Ru by Zr, Mo, and Mn ions was performed considering that: a) the magnetic effect of the doped ions; and b) the difference of the ionic radii and the hetero-valence of the Zr, Mo, and Mn ions. According to previous studies, it was reported that the physical properties of this system are very sensitive even when the concentration of the doping in the cation sites is very small [6-13]. For this reason, we have substituted 10 % of ruthenium by other metallic cation in order to obtain monophase samples. The aim of this investigation was to synthesize the monophase of $\text{Ru}_{0.9}\text{M}_{0.1}\text{Sr}_2\text{GdCu}_2\text{O}_8$ with

M = Zr, Mo, and Mn samples via the solid-state reaction method and study the influence of the metal ions type on the structural and superconducting properties.

2. EXPERIMENTAL PROCEDURE

2.1. Synthesis

Polycrystalline samples of the $\text{Ru}_{0.9}\text{M}_{0.1}\text{Sr}_2\text{GdCu}_2\text{O}_8$ system with M = Zr, Mo, and Mn, were synthesized by the solid-state reaction method at ambient pressure. The starting materials were RuO_2 (99.9%, CERAC), ZrO_2 (Riedel-de Haën pure), MoO_3 (99.5%, ALDRICH), MnO (99.99%, ALDRICH), SrCO_3 (99.5%, CERAC), Gd_2O_3 (99.99%, STREM), and CuO (99.99%, ALDRICH).

Structure and purity of the starting materials were determined by XRD. Prior to weighing, SrCO_3 was preheated for 10-20 minutes at 120 °C in order to dehydrate it. The stoichiometric mixture of the starting materials was done in air for 30 minutes, grinded with an agate mortar, resulting in homogenous slurry, pressed, and treated as follows: 1) mixing and grinding in an agate mortar and 2) calcination at temperature ranging from 960°C to 1020 °C for 24 h. These steps were repeated five times. 3) The resulting polycrystals were then pressed into circular pellets (13 mm) and sintered using temperatures between 1050 and 1055 °C for 5 days in a tubular furnaces with flowing oxygen and then slowly cooled down to room temperature.

2.2.Characterization

The X-ray powder diffraction (XRD) patterns of $\text{Ru}_{0.9}\text{M}_{0.1}\text{Sr}_2\text{GdCu}_2\text{O}_8$ samples, with M = Zr, Mo, and Mn were obtained with an APD 2000 PRO X-Ray diffractometer with Cu K α radiation. Measurements were done in 2 θ range of 2° to 70° with a scanning step width of 0.025° and a 15 s scanning time per step. The Rietveld method using the Full Prof program was carried out for the refinement of the crystal structures. The morphology and chemical analysis of the materials were determined using a scanning electron microscope, (SEM) combined with an X-ray energy dispersive

spectrometer (SEM/EDS HITACHI S-3400N). Low temperature dc resistance measurement were performed using the standard four-probe method from room temperature down to 8K [14].

3. RESULTS AND DISCUSSION

Fig. 1 shows the XRD pattern of the pure and doped samples with nominal composition $\text{Ru}_{0.9}\text{M}_{0.1}\text{Sr}_2\text{GdCu}_2\text{O}_8$ (M = Ru, Zr, and Mo). XRD measurements confirm the formation of pure phase for M = Ru and Mn, whereas for samples with M = Zr and Mo, small additional peaks are observed. These additional reflections are attributed to the formation of the SrRuO_3 impurity [2]. Moreover, X-ray diffraction patterns of all doped samples revealed the same primitive tetragonal structure of the undoped $\text{RuSr}_2\text{GdCu}_2\text{O}_8$ compound (Fig. 1).

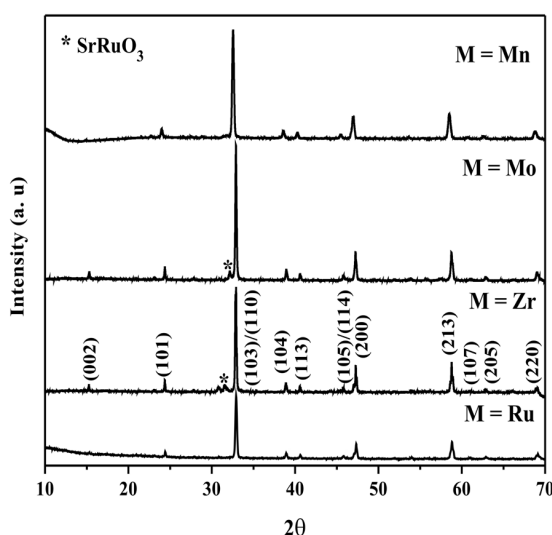


Fig. 1. XRD patterns of the $\text{Ru}_{0.9}\text{M}_{0.1}\text{Sr}_2\text{GdCu}_2\text{O}_8$ (M = Ru, Zr, Mo, and Mn) system.

Fig. 2 shows the SEM micrographs of the $\text{Ru}_{0.9}\text{M}_{0.1}\text{Sr}_2\text{GdCu}_2\text{O}_8$ system with M = Ru, Zr, Mo, and Mn. As it can be seen, the samples show similar characteristics in their morphology and are porous with different grain sizes, from 1 up to 5 μm . The semi-fusion always is present, depending of the metal.

EDX analysis was performed to verify the chemical composition of the samples. Different regions of the surface in each sample were ana-

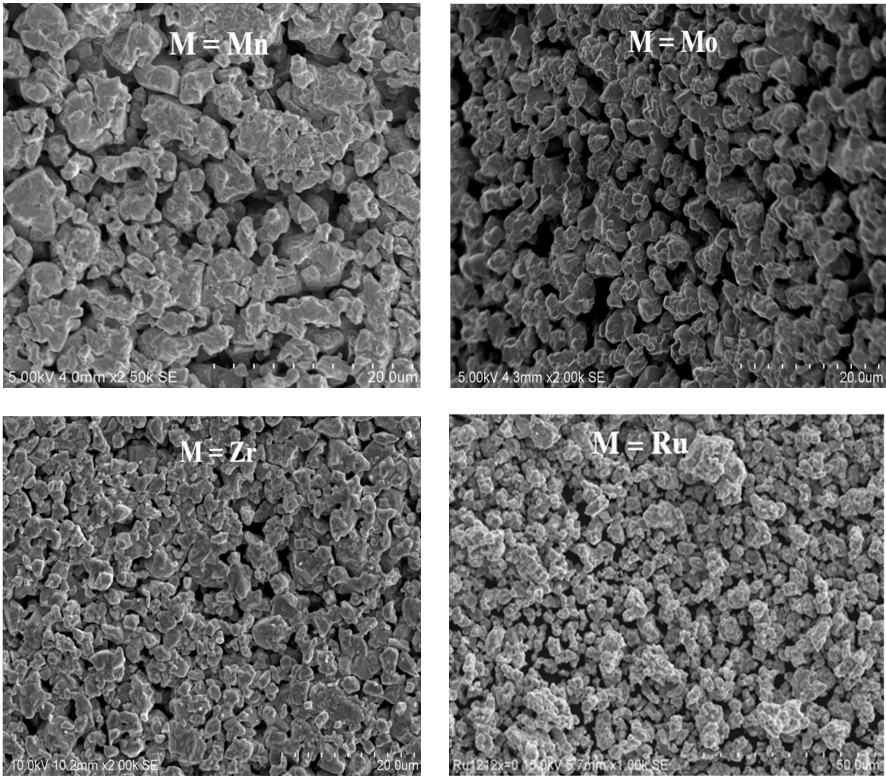


Fig. 2. SEM micrographs of the Ru_{0.9}M_{0.1}Sr₂GdCu₂O₈ system, with M = Ru, Zr, Mo, and Mn.

lyzed and an average was taken. The results are present in Table 1. The experimental and expected atomic percentage is similar within 6wt% [15-17].

EDX permits the determination of chemical composition of pure and doped samples [18, 19]. The structure analysis of all samples was performed using the Rietveld refinement. It was taken into account the possibility that M = Zr, Mo, and Mn can also occupy the Ru ion sites. The presence of the SrRuO₃ compound as a secondary phase was included with space group (S.G.) P4/mmm (No. 123). Ru, Zr, Mo, and Mn ions occupy

the crystallographic 1b sites (0, 0, 0.5); Gd ions, the 1c sites (0.5, 0.5, 0); Sr ions, the Wyckoff position 2 h(0.5, 0.5, z); Cu, the 2g position (0, 0, z); and the oxygen ions, distributed among the 8 s(x, 0, z), the 4 o(x, 0.5, 0.5) and the 4 i(0, 0.5, z) positions. The oxygen sites in the SrO, CuO₂, and RuO₂ planes are denoted by O(1), O(2) and O(3), respectively.

Tables 2 presents the results of the refinement of the bond angles, bond lengths, and cell parameters of the Ru_{0.9}M_{0.1}Sr₂GdCu₂O₈ system with M = Ru, Zr, Mo and Mn. The crystallograph-

Table 1. Chemical composition analysis results of Ru_{0.9}M_{0.1}Sr₂GdCu₂O₈ (M = Ru, Zr, Mo and Mn)

Ru _{0.9} M _{0.1} Sr ₂ GdCu ₂ O ₈	(wt%)					
	Ru	M	Sr	Gd	Cu	O
RuSr ₂ GdCu ₂ O ₈	6.42	----	14.28	7.14	14.28	57.14
Ru _{0.9} Zr _{0.1} Sr ₂ GdCu ₂ O ₈	5.65	1.18	13.76	7.37	13.87	58.17
Ru _{0.9} Mo _{0.1} Sr ₂ GdCu ₂ O ₈	5.98	1.76	14.06	7.89	14.07	56.24
Ru _{0.9} Mn _{0.1} Sr ₂ GdCu ₂ O ₈	5.87	0.98	13.51	7.23	13.89	57.80

Table 2. Cell parameters, bond lengths (nm), and bond angles (deg) for $\text{Ru}_{0.9}\text{M}_{0.1}\text{Sr}_2\text{GdCu}_2\text{O}_8$ (M = Ru, Zr, Mo, and Mn) system.

Structural parameters	$\text{Ru}_{0.9}\text{M}_{0.1}\text{Sr}_2\text{GdCu}_2\text{O}_8$			
	M=Mo	M=Ru	M=Mn	M=Zr
a(nm)	0.3840	0.3850	0.3858	0.3860
c(nm)	1.1550	1.1589	1.1590	1.1604
V(nm ³)	0.1703	0.1718	0.1725	0.1729
Ru-O(3)-Ru	152.56	152.56	152.56	152.56
Cu-O(2)-Cu	167.02	166.68	166.60	166.67
Cu-O(1)-Ru	169.01	169.70	169.93	169.05
Ru-O(1) (nm)	0.1949	0.1968	0.2082	0.2091
Ru-O(3) (nm)	0.9979	0.19978	0.19984	0.19987
Cu-O(1) (nm)	0.19893	0.19968	0.2282	0.23931

ic parameter values showed in Table 2 for undoped and doped samples are in agreement with previous published results [20]. From the refinement results, it is noted that all metals ions occupy both the Ru and Cu sites. Fig. 3 shows the variation of the structural parameters of the

$\text{Ru}_{0.9}\text{M}_{0.1}\text{Sr}_2\text{GdCu}_2\text{O}_8$ system as a function of ionic radius of M = Ru, Zr, Mo, and Mn. It can be observed that the partial substitution of Ru^{4+} by Mn^{2+} and Zr^{4+} is accompanied by an increase of lattice cells (a and c) as well as Ru – O(1) and Cu– O(1) bond lengths. This result refers to the

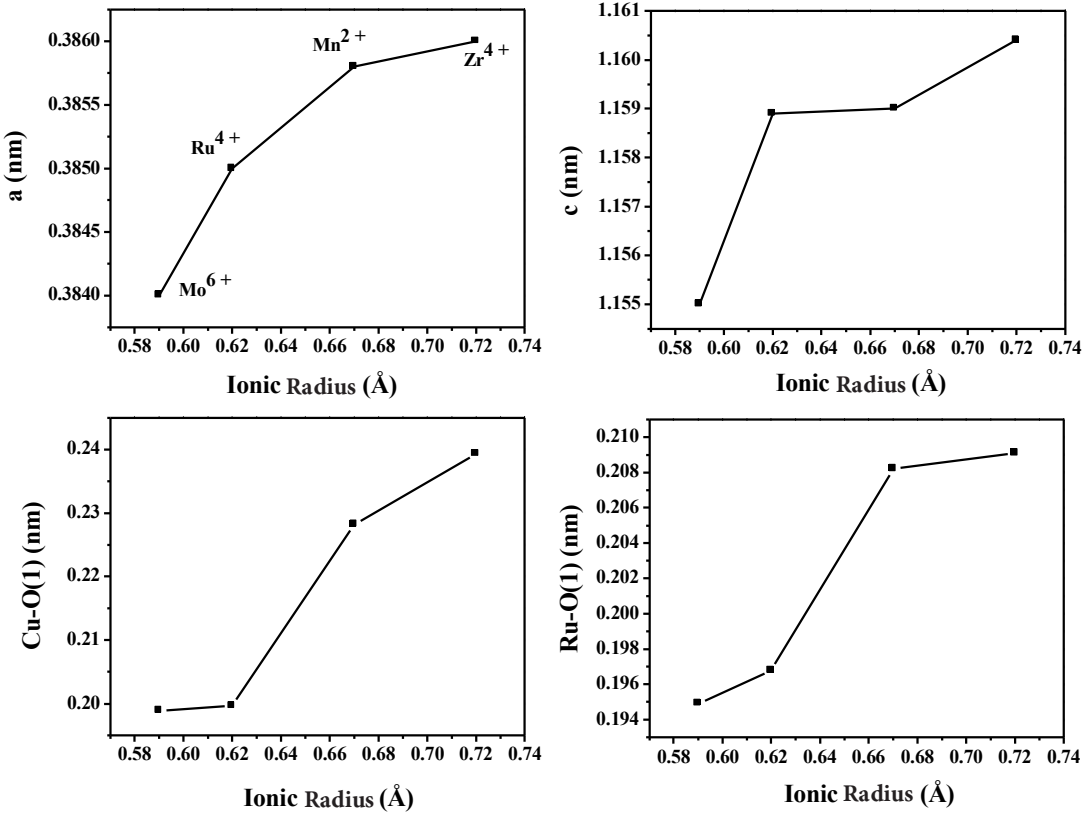


Fig. 3. Variation of Cu-O(1) and Ru-O(1) bond lengths vs. the ionic radius of Ru, Zr, Mo, and Mn.

fact that the ionic radii of the Mn^{2+} and Zr^{4+} ions are larger than that of Ru^{4+} ($\text{IR}^{\text{VI}} \text{Ru}^{4+} = 0.62 \text{ \AA}$, $\text{IR}^{\text{VI}} \text{Mn}^{2+} = 0.67 \text{ \AA}$ and $\text{IR}^{\text{VI}} \text{Zr}^{4+} = 0.72 \text{ \AA}$) [21]. The decrease in lattice parameters with the substitution of Ru^{4+} ions by the Mo^{6+} ions is attributed to the smaller ionic radii of Mo in comparison to the Ru ions in the hexagonal coordination state ($\text{IR}^{\text{VI}} \text{Mo}^{6+} = 0.59 \text{ \AA}$) [21].

On the other hand, the refinement indicates that Ru-O(1)-Cu bond angle for $\text{M} = \text{Ru}$, Zr, Mo and Mn samples show an insignificant change compared with the pristine $\text{RuSr}_2\text{GdCu}_2\text{O}_8$ compound. This parameter presents the deviation of the apical oxygen O(1) along the plane perpendicular to the c-axis. The Ru-O(3)-Ru bond angle, which is a measure of the rotation of the RuO_6 octahedra around the c-axis, remains extraordinarily constant. The Cu-O(2)-Cu bond angle, which is a measure of the buckling of the CuO_2 layer, shows a slight dependence with the ionic radii of the Zr, Mo, and Mn ions.

Fig. 4 shows the normalized resistance as a

function of temperature for pristine $\text{RuSr}_2\text{GdCu}_2\text{O}_8$ compound and the $\text{M} = \text{Zr}$, Mo, and Mn modified samples. It can be observed that for $\text{M} = \text{Ru}$ and Zr, the decreasing of temperature is accompanied by a slight increasing of the resistance until a maximum value, whereas the onset of superconductivity transition is observed at around 30 K; zero resistance is achieved at around 11 K. Furthermore, as can be seen in Fig. 4 for $\text{M} = \text{Ru}$, the superconducting transition width is comparable to that observed in $\text{RuSr}_2\text{GdCu}_2\text{O}_{8.21}$ [22,23]. Part of the superconducting transition width may be attributed to oxygen disorder in $\text{Ru}_{0.9}\text{Zr}_{0.1}\text{Sr}_2\text{GdCu}_2\text{O}_8$ and structural disorder in $\text{RuSr}_2\text{GdCu}_2\text{O}_8$ [24]. For $\text{M} = \text{Mo}$ and Mn, the normalized resistance curves decrease with increasing of temperature until a relative minimum is observed around 82 K, then increase just before the onset of transition of temperature around 33 K without any signal of a superconducting transition. The substitution of 10 % of the Ru ions by Mn and Mo ions suppressed the superconductivity. The absence

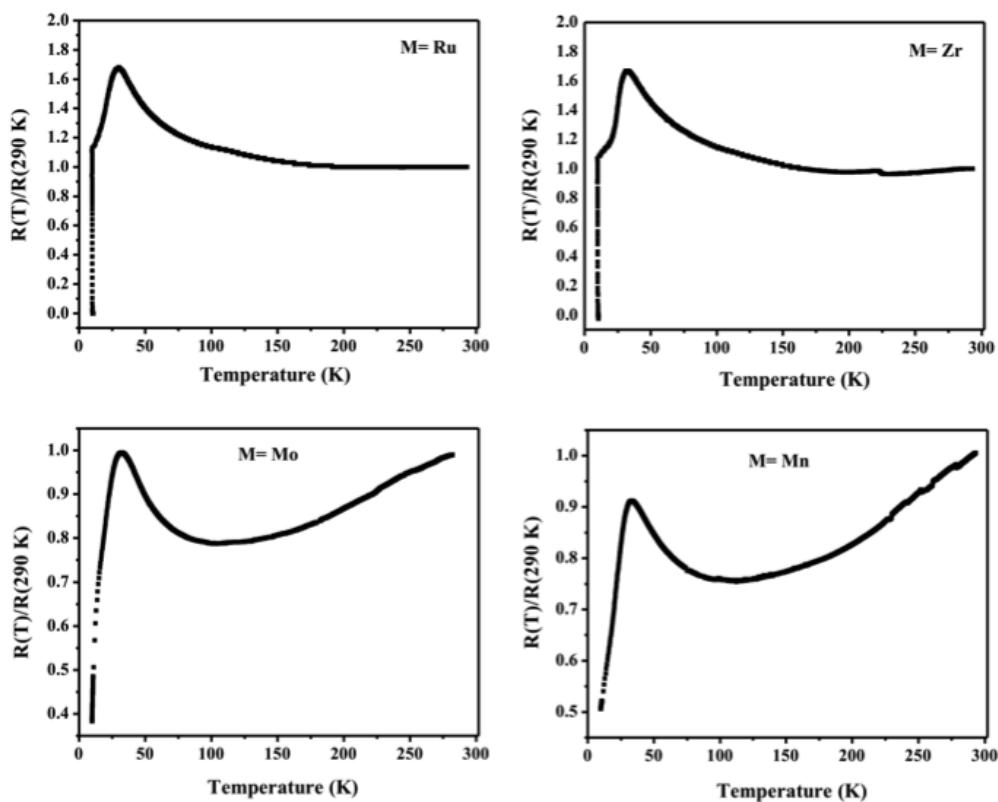


Fig. 4. Normalized resistance as a function of temperature of the $\text{Ru}_{0.9}\text{M}_{0.1}\text{Sr}_2\text{GdCu}_2\text{O}_8$ system, with $\text{M} = \text{Ru}$, Zr, and Mn.

of superconductivity in these samples can be explained by the Mn and Mo doping, combined with a pair-breaking effect [26,27] caused by weak coupling between the carriers in CuO_2 and RuO_2 layers. This suggestion may be due to oxygen depletion by the possible partial substitution of Mn and Mo atoms in CuO_2 and RuO_2 layered. Rietveld-refinement results showed in Table 2 and Fig. 3 confirm this possibility.

4. CONCLUSION

We successfully substituted 10% of the Ru ions by Zr, Mo, and Mn ions in the $\text{Ru}_{0.9}\text{M}_{0.1}\text{Sr}_2\text{GdCu}_2\text{O}_8$ system. XRD diffractograms showed that all samples present a similar pattern. It was found that cell parameters (a and c) as well as the Cu-O(1) and Ru-O(1) bond lengths increase by increasing the ionic radii of Mo, Mn, and Zr ions doped. The absence of superconductivity in these samples were attributed to the Mn and Mo substitution, combined with a pair-breaking effect caused by weak coupling between the carriers in the CuO_2 layers and the RuO_2 layers.

ACKNOWLEDGMENT

The authors acknowledge the financial support provided by CONACyT Grant No. CB-169133.

REFERENCES

1. Lebedev, O. I., Van Tendeloo, G., Cristiani, G., Habermeyer, H. U. and Matveev, A. T., "Structure-properties relationship in ferromagnetic superconducting $\text{RuSr}_2\text{GdCu}_2\text{O}_8$. Phys." Rev. B, 2005, 71, 134523, 1-8.
2. Bauernfeind, L., Widder, W. and Braun, H. F., "Ruthenium-based layered cuprates $\text{RuSr}_2\text{LnCu}_2\text{O}_8$ and $\text{RuSr}_2(\text{Ln}_{1-x}\text{Ce}_x)\text{Cu}_2\text{O}_{10}$ (Ln= Sm, Eu and Gd)." Physica C: Superconductivity, 1995, 254, 151-158.
3. Felner, I., Asaf, U., Reich, S., and Tsabba, Y., "Magnetic properties of $\text{RSr}_2\text{RuCu}_2\text{O}_{8+\delta}$ (R= Eu and Gd)". Physica C: Superconductivity, 1999, 311, 163-171.
4. Dabrowski, B., Klamut, P. W., Maxwell, M., Mini, S. M., Kolesnik, S., Mais, J., Shengelaya, A., Khazanov, R., Keller, H., Sulkowski, C., Wlosewicz, D. and Matusiak, M., "Superconductivity and magnetism in pure and substituted $\text{RuSr}_2\text{GdCu}_2\text{O}_8$." J. superconductivity, 2002, 15, 439-445.
5. Parthiban, P. and Balamurugan S., "Synthesis Micro-Structural and FT-IR Studies of Ball Milled-Annealed Nanocrystalline Ruthenocuprate, $\text{RuSr}_2\text{EuCu}_2\text{O}_{8-\delta}$." Adv. Sci., Eng. Med., 2015, 7, 506-509.
6. Balamurugan, S., "Impact of Ce doping on the magnetic and transport properties of $\text{Y}_{1-x}\text{Ce}_x\text{Sr}_2\text{Ru}_{0.9}\text{Cu}_{2.1}\text{O}_{7.9}$; $x=0.05$ and 0.1 ." Inter. J. Mod. Phys. B, 2012, 26, 1250157, 1-13.
7. Malo, S., Ko, D., Rijssenbeek, J. T., Maignan, A., Pelloquin, D., Dravid, V. P. and Poeppelmeier, K. R., "Coexistence of superconductivity and ferromagnetism in $1212\text{-Ru}_{1-x}\text{M}_x\text{Sr}_2\text{GdCu}_2\text{O}_8$ (M=Ti, V, Nb)." Int. J. Inorg. Mater., 2000, 2, 601-608.
8. Steiger, M., Kongmark, C., Rueckert, F., Harding, L. and Torikachvili M. S., "Pressure study of superconductivity and magnetism in pure and Rh-doped $\text{RuSr}_2\text{GdCu}_2\text{O}_8$ materials." Physica C: Superconductivity, 2007, 453, 24-30.
9. Dos Santos-García, A. J., Arévalo-López, Á. M., Fernández-Sanjulián, J., Alario-Franco, M. Á. and Frost, D., "Synthesis, structural and magnetic disordering in the $\text{IrSr}_2\text{RECu}_2\text{O}_{8+x}$ family of metalocuprates by HP+HT oxidation." High Pressure Res., 2010, 30, 17-23.
10. Chen, X. H., Sun, Z., Wang, K. Q., Xiong, Y. M., Yang, H. S., Wen, H. H., Ni, Y. M. and Zhao, Z. X., "Superconductivity and specific heat of $\text{Ru}_{1-x}\text{TaxSr}_2\text{GdCu}_2\text{O}_8$ and $\text{RuSr}_2\text{Gd}_{1.4}\text{Ce}_{0.6}\text{Cu}_2\text{O}_y$." J. Phys. Condens. Matter, 2000, 12, 10561-10569.
11. Escamilla, R., Morales, F., Akachi, T. and Gómez R., "Study of the crystal structure, superconducting and magnetic properties of $\text{Ru}_{1-x}\text{FexSr}_2\text{GdCu}_2\text{O}_8$." Supercond. Sci. Technol., 2005, 18, 798-804.
12. Balamurugan, S., "Detailed Physical Characterizations of Cu-rich and Ru poor ($\text{Ru}_{0.9}\text{Cu}_{0.1}\text{Sr}_2\text{YCu}_2\text{O}_{7.9}$)." J. Sup. Nov. Mag., 2010, 23, 1359-1367.
13. Yang, L. T., Liang, J. K., Liu, Q. L., Song, G. B., Liu, F. S., Luo, J. and Rao, G. H., "Effect of Co substitution on superconductivity and magnetic order in $\text{RuSr}_2\text{GdCu}_2\text{O}_8$." Physica C: Superconductivity, 2004, 403, 177-182.
14. García-Vázquez, V., Pérez-Amaro, N., Canizo-Cabrera, A., Cumplido-Espíndola, B., Martínez-Hernández, R. and Abarca-Ramírez, M. A., "Selected error sources in resistance measurements on superconductors." Rev. Sci. Instrum., 2001, 72, 3332-3339.

15. Beaman, D. R. and Isasi, J. A., "Electron Beam Microanalysis," Part I: Fundamentals and Applications, ed. American Society for Testing and Materials, Philadelphia, 1972, 23–24.
16. Garcia-Vazquez, V., Abatal, M., Oubrame, O., Alfonso, I., Alazki, H., Flores-Flores, J. O., Quiroz, A., Flores-García, J. O. and Gonzalez, G., "Interrelation between structural and electrical properties in $\text{RuSr}_2\text{GdCu}_2\text{O}_{8\pm z}$ prepared under different annealing conditions." *IEEE Trans. Appl. Supercond.*, 2017, 27, 1-3.
17. Quiroz, A., Chavira, E., Garcia-Vazquez, V., Gonzalez, G. and Abatal, M., "Structural, electrical and magnetic properties of the pyrochlore $\text{Er}_{2-x}\text{Sr}_x\text{Ru}_2\text{O}_7$ ($0 \leq x \leq 0.10$) system." *Rev. Mex. Fis.*, 2018, 64, 222–227.
18. Güner, S., Auwal, I. A., Baykal, A. and Sözeri, H., "Synthesis, characterization and magneto optical properties of $\text{BaBixLaxYxFe}_{12-3x}\text{O}_{19}$ ($0.0 \leq x \leq 0.33$) hexaferrites." *J. Magn. Magn. Mater.*, 2016, 416, 261-268.
19. González-Rivera, Y. A., Meza-Rocha, A. N., Aquino-Meneses, L., Jiménez-Sandoval, S., Rubio-Rosas, E., Caldiño, U., Álvarez, E., Zelaya-Angel, O., Toledo-Solano, M. and Lozada-Morales, R., "Photoluminescent and electrical properties of novel Nd^{3+} doped ZnV_2O_6 and $\text{Zn}_2\text{V}_2\text{O}_7$." *Ceram. Int.*, 2016, 42, 8425-8430.
20. Chmaissem, O., Jorgensen, J. D., Shaked, H., Dollar, P. and Tallon, J. L., "Crystal and magnetic structure of ferromagnetic superconducting $\text{RuSr}_2\text{GdCu}_2\text{O}_8$." *Phys. Rev. B*, 2000, 61, 6401-6407.
21. Shannon, R. D., "Revised effective ionic radii and systematic studies of interatomic distances in halides and chalcogenides." *Acta crystallogr. A: crystal physics, diffraction, theoretical and general crystallography*, 1976, 32, 751-767.
22. Požek, M., Dulčić, A., Paar, D., Williams, G. V. M. and Krämer, S., "Transport and microwave study of superconducting and magnetic $\text{RuSr}_2\text{EuCu}_2\text{O}_8$." *Phys. Rev. B*, 2001, 64(6), 064508, 1-7.
23. Yamaki, K., Bamba, Y. and Irie, A., "Preparation of fine single crystals of magnetic superconductor $\text{RuSr}_2\text{GdCu}_2\text{O}_{8-\delta}$ by partial melting." *Jpn. J. App. Phys.*, 2018, 57, 033101, 1-5.
24. Williams, G. V. M. and Ryan, M., "Raman transport and magnetization study of the $\text{RuSr}_2\text{R}_{2-x}\text{Ce}_x\text{Cu}_2\text{O}_{10+\delta}$ ($\text{R}=\text{Gd}, \text{Eu}$) high-temperature superconducting cuprates." *Phys. Rev. B*, 2001, 64, 094515, 1-8.
25. Yamaki, K., Mochiku, T., Funahashi, S., Bamba, Y., Kitamura, M., Matsushita, Y. and Irie, A., "Synthesis and structural characterization of a superconducting $\text{GdSr}_2\text{RuCu}_2\text{O}_{8-\delta}$ single crystal grown by partial melting." *Appl. Phys. Express*, 2018, 11, 113-101.
26. Kumar, A. and Awana, V. P. S., "Impact of Mn Substitution at Ru Site in $\text{RuSr}_2(\text{Eu}_{1.4}\text{Ce}_{0.6})\text{Cu}_2\text{O}_{10-\delta}$ Magneto-Superconductor." *J. Supercond. Nov. Magn.*, 2011, 24, 499-504.
27. Kuz'micheva, G. M., Andreenko, A. S., Kostyleva, I. E., Zalevski, A. and Warchulska, J., "Synthesis, structure, superconducting and magnetic properties of $(\text{Ru}_{5+1-x}\text{Mo}_{6+x})(\text{Sr,Gd})_2(\text{Gd}_{0.7}\text{Ce}_{4+0.3})_2\text{Cu}_2\text{O}_{10}$ ($x=0.0, 0.25, 0.50, 0.75, 1.0$)." *Physica C: Superconductivity*, 2003, 400, 7–18.